Plant Physiology and Biochemistry 144 (2019) 345–354

Contents lists available at ScienceDirect

Plant Physiology and Biochemistry

journal homepage: www.elsevier.com/locate/plaphy

Research article

Boron and calcium deficiency disturbing the growth of trifoliate rootstock seedlings (*Poncirus trifoliate* L.) by changing root architecture and cell wall

Yalin Liu, Muhammad Riaz, Lei Yan, Yu Zeng, Jiang Cuncang*

Microelement Research Center, College of Resources and Environment, Huazhong Agricultural University, Wuhan, Hubei, 430070, PR China

ARTICLE INFO

Keywords:
Boron
Calcium
Root architecture
Cell wall
Pectin
Poncirus trifoliate L

ABSTRACT

Boron (B) and calcium (Ca) are essential elements for plant growth. Both deficiencies inhibit root growth. However, the mechanism of inhibition is not well clear. Morphological characteristics of roots and changes in root cell wall grown at different B and Ca deficiencies were examined by using a hydroponic culture system. Both B and Ca deficiencies caused reduced plant biomass and root growth. Ca deficiency significantly decreased the fresh weight of root, stem, and leaves by 47%, 50%, and 62%, respectively, while B deficiency only reduced root fresh weight. The PCA combined with Pearson correlation analysis showed that there was significant different correlation among root parameters under B and Ca deficiency treatments when compared to control. The results of observation of transmission electron microscope showed that Ca deficiency reduced but B deprivation increased the thickness of the cell wall. Combining these technologies like X-ray diffraction, fourier transform infrared spectroscopy, homogalacturonan epitopes (JIM5 and JIM7), we confirmed that those changes above may be due to different changes in the degree of methyl esterification of pectin and glycoprotein of the cell wall. Taken together, we concluded that B deficiency can promote the formation of more low methyl esterified pectin to increase cell wall thickness, and then affect the morphological development of root system, while the formation of more highly methyl esterified pectin to increase cell wall degradation under Ca deficiency, which inhibited root elongation and formation of root branches.

1. Introduction

Boron (B) and calcium (Ca) are crucial for plants in completing life cycle by promoting their physiological and biochemical functions (Brown et al., 2002; Tuteja, 2009). There is a relatively stable mechanism for B and Ca levels *in vivo* plants. Previous studies showed that these two elements are closely related to each other, and the deprivation or excess of one element affects the nutritional status of the others (Agustín et al., 2014; Herrera, 2013; Piñero et al., 2017; Tariq and Mott, 2007).

The relationship between B and Ca has been extensively studied (Goldbach et al., 2015). Early studies on tomato plants showed that increase of Ca supply in culture solution aggravated B deficiency symptoms, and translocation of Ca was different between lower and upper leaves under B deficiency condition (Yamauchi et al., 1986). In *Arabidopsis thaliana* roots, the level of cytosolic Ca^{2+} was more pronounced under B deprivation (Quiles-Pando et al., 2013), while B toxicity symptoms of sweet pepper (*Capsicum annuum* L.) was effectively alleviated by the additional application of Ca (María et al., 2017). This may be due to the synergistic physiological effects of B and Ca in plants and both these elements are necessary components of the cell wall (CW). The Ca also has hormone-like effects in regulating nutrient uptake by roots (Siddiqui et al., 2013). Several reports described that B deficiency affected genes expression that could be regulated by Ca^{2+}, suggesting the effect of B on Ca^{2+}-mediated signaling pathways (Redondo-Nieto et al., 2012; Agustín et al., 2014).

The CW matrix of higher plants contains mainly polysaccharides like cellulose, hemicellulose, and pectin, which affects wall strength and flexibility, and presents a physical barrier to potentially adverse environmental conditions (Tan et al., 2013; Bénédicte et al., 2019). Previous studies have shown that B–Ca interaction with respect to cell wall stability (Bastias et al., 2010). Pectic polysaccharides are a group of polymers containing α-1,4-D-galacturonic acid (GalA) residues (O'Neill et al., 1990). B plays an important role in CW structural integrity by cross-linking rhamnogalacturonan II (RG-II) in pectin polysaccharides (Kobayashi et al., 1996), which deficiency significantly results in the increase of root CW extraction ratio and root CW thickness (Wu et al., 2017). Meantime, B deficiency inhibits the growth of primary and lateral roots by limiting cell division in apical growth areas and by the disorganized distribution of CW (Ishii and Matsunaga, 2001;

* Corresponding author.
E-mail address: jcc2000@mail.hzau.edu.cn (J. Cuncang).

https://doi.org/10.1016/j.plaphy.2019.10.007
Received 14 August 2019; Received in revised form 5 October 2019; Accepted 5 October 2019
Available online 07 October 2019

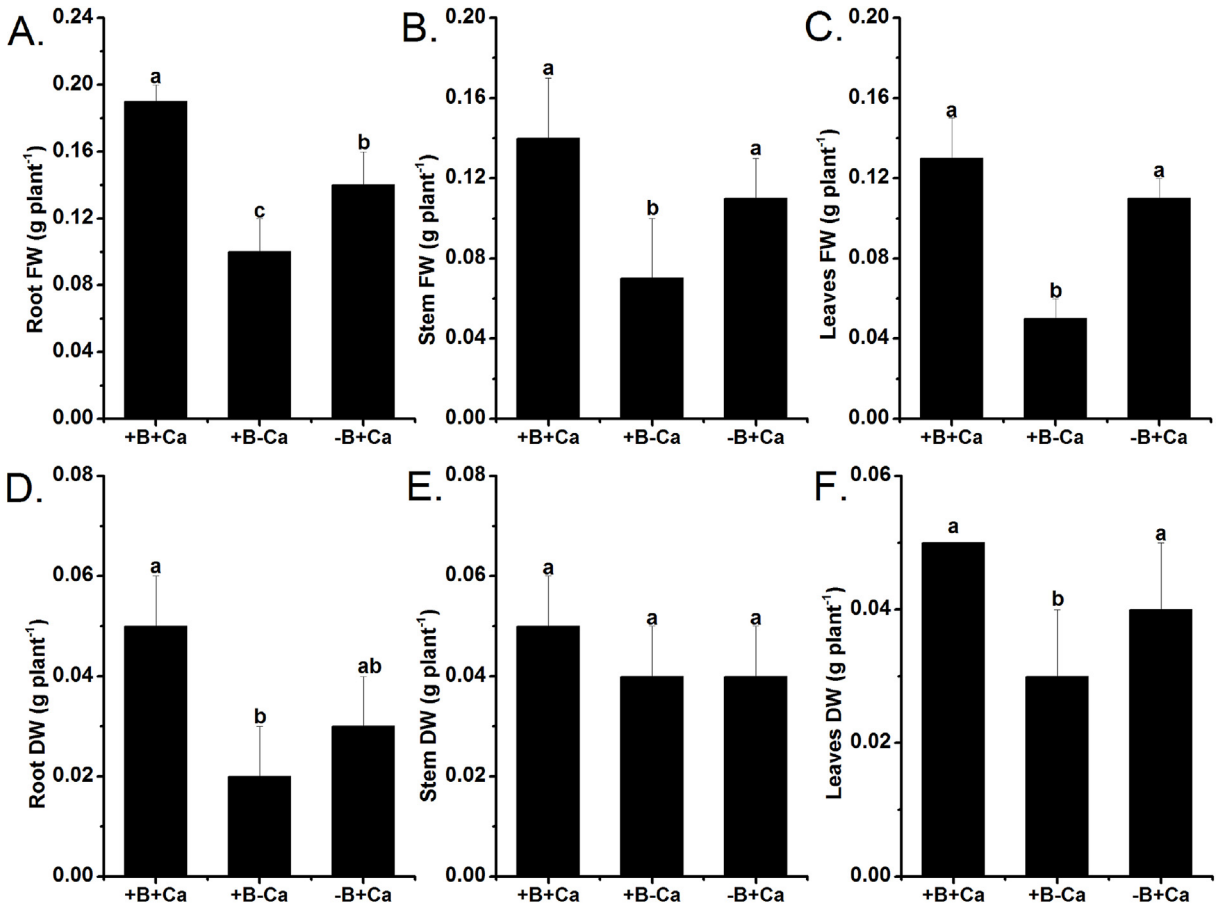

Fig. 1. Effect of B or Ca deficiency on the growth characteristics of trifoliate rootstock (*Poncirus trifoliate* L.). +B + Ca: control, +B–Ca: Ca deficiency, -B + Ca: B deficiency. DW: dry weight; FW: fresh weight. Different lowercase letters in the figure indicate a significant difference among three treatents at $P < 0.05$ level with mean ± SD (Duncan's multiple comparison test).

Martín-Rejano et al., 2011; Riaz et al., 2018). Ca^{2+} forms ionic cross-links with some carboxylates of GalA residues in homogalacturonan (HG), the Ca^{2+}-dependent ionic cross-linking of HG and the covalent cross-linking of B-RG-II form a stable three-dimensional pectic network to maintain the mechanical strength of CW while GalA residues in methyl esterification of HG may bind through hydrophobic interaction (O'Neill et al., 2004). When cells were deprived of Ca^{2+}, some degradation in cell-wall structure had occurred by interfering with the deposition of acidic pectic polymers on cell walls (Konno et al., 2010). Additionally, Ca deficiency also affects the root architecture by suppressing axial root elongation and (or) lateral root (Cao et al., 2013).

In China, citrus production occupies an important position and trifoliate rootstock seedlings (*Poncirus trifoliate* L.) are widely planted in the main citrus-producing areas. The root architecture of trifoliate rootstock has a direct influence on the yield and quality of citrus. Nevertheless, due to heavy rainfall, the soil in this area is becoming more acidic, leading to the depletion of available B and Ca. Both deficiencies of these elements had greatly limited plant root growth. However, the different mechanism of inhibition is not well understood especially in trifoliate rootstock seedlings (Jiang et al., 2009; Cao et al., 2013; Kunhikrishnan et al., 2016). Therefore, we conducted this experiment to explore the difference in root growth inhibition under B and Ca deficiency by studying the root growth characteristics and variations in CW components.

2. Materials and methods

2.1. Experimental design, plant material, and treatments

Seeds of trifoliate orange (*Poncirus trifoliate* (L.) Raf.), obtaining from the local market, were surface sterilized with 5% sodium hypochlorite for 15 min, and then rinsed with double distilled water (DDW). Seeds were sown in plates (50 cm long, 15 cm wide and 4 cm height) filled with fine quartz sand and irrigated with 30 mL of DDW (24-h dark and 30 °C) every day. After two weeks, when the seedlings emerged, they were cultured with modified Hoagland and Arnon (1950) solution; 2 mM KNO_3, 0.5 mM $MgSO_4{\cdot}7H_2O$, 1.23 mM $Ca(NO_3)_2$, 0.14 mM Na_2HPO_4, 0.32 mM NaH_2PO_4, 4.45 μM $MnCl_2$, 0.8 μM $ZnSO_4$, 0.16 μM $CuSO_4$, 0.18 μM Na_2MoO_4, 10 μM H_3BO_3, and 28.7 μM Fe-EDTA, at 25% for seven days, 50% for another seven days and 100% for another seven days until transplantation. Then, seedlings were grown in a greenhouse in 16-L pots, and the nutrient solution was replaced every seven days until harvest (about 21 days). The pots were arranged in a simple randomized design with three treatments: +B + Ca, +B–Ca, and -B + Ca. The Ca-deficient medium was made by replacing 1.23 mM $Ca(NO_3)_2$ with 1.23 mM NH_4NO_3 while B-free medium was obtained by removing the only source of H_3BO_3.

2.2. Measurement of plant biomass and root morphological characteristics

At the end of the experiment, four seedlings from each treatment were collected and separated into roots, stem, and leaves, for measuring fresh weight (FW). The roots were scanned by root analyzer (Epson Perfection V700), and data were analyzed by WinRHIZO root analysis

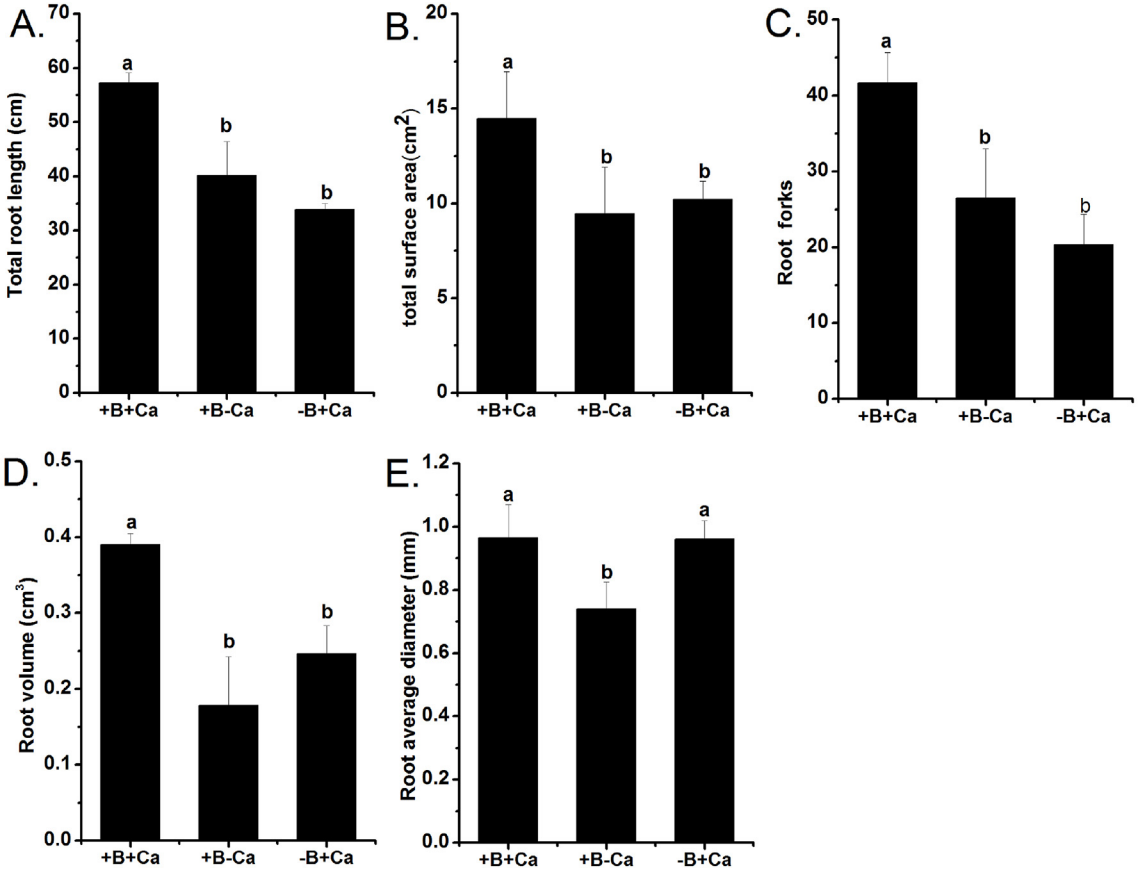

Fig. 2. Effect of B or Ca deficiency treatment on the root morphological parameters of trifoliate rootstock (*Poncirus trifoliate* L.). +B + Ca: control, +B–Ca: Ca deficiency, -B + Ca: B deficiency. Different lowercase letters in the figure indicate a significant difference among three treatments at $P < 0.05$ level with mean ± SD (Duncan's multiple comparison test).

system. The measured parameters included total root length (TRL), total surface area (TSA), root forks (RFs), root volume (RV) and root average diameter (RAD). The samples were subsequently oven-dried at 75 °C until constant weight for the determination of the dry weights (DW). Root length ratio (RLR), root fineness (RF), root mass ratio (RMR) and root tissue density (RTD) were calculated by following equations (Ali et al., 2018):

RLR = total root length/whole plant dry weight (cm g^{-1}).
RF = total root length/root volume (cm cm^{-3}).
RMR = root dry weight/whole plant dry weight (g g^{-1}).
RTD = root dry weight/root volume (g cm^{-3}).

2.3. Transmission electron microscope (TEM) of roots

The TEM slides of roots were prepared as described by Wu et al. (2017). Briefly, the samples (the part of 1 cm from root tip) were fixed in phosphate buffer solution (PBS) containing 2.5% glutaraldehyde at 4 °C overnight. The samples were prefixed in 1% OsO4 in PBS at 4 °C overnight and dehydrated through a series of ethanol concentrations. Then, the paraffin-embedded roots were cut into small pieces, subsequently, ultrathin sections were stained with 2% uranyl acetate and lead citrate, and examined with a TEM (Hitachi 500 electron microscope) at 80 kV. The CW thickness was measured by a ruler tool in Adobe Photoshop CS6.

2.4. Extraction of the roots CW

The 3 g fresh root samples were homogenized by a mortar and pestle with liquid nitrogen. The homogenate was washed with ice-cold ultrapure water (10 vol) and centrifuged (5000 × *g*, 10 min), and the supernatant was discarded. The residue was then washed with 10 vol of ice-cold water and recentrifuged (3000 × *g*, 10 min). The residue was washed with 10 vol of 80% ethanol for three times to remove chlorophyll and sugars, and 10 mL methanol: trichloromethane (1:1, v/v) once to remove sugars and lipids, then rinsed with 10 mL of acetone once and dried at 50 °C. The dried insoluble pellet was defined as CW, and the CW extraction rate was obtained by the calculation of the dry weight of root cell wall (g) per the fresh weight of root (g) (Hu and Brown, 1994; Liu et al., 2014).

2.5. Measurement of X-ray diffraction (XRD) of root CW

The root CW samples (50 mg) was employed for XRD analysis by X-ray diffractometer (D8 Advance, Bruker, Germany) at 40 kV and a current of 40 mA by using CuKα radiation source with a wavelength of 0.2 nm. The scanning of the diffraction angle (2θ) from 5° to 30° was conducted at a scanning speed of 5° min^{-1}. Crystallite size was calculated by the modified Scherrer Eq. (1) using a similar procedure reported by Szymanska-Chargot et al. (2017):

$$d = \frac{0.9\lambda}{\cos\theta \times FWHM} \quad (1)$$

where λ is the X-ray wavelength (0.2 nm), FWHM is the full width at half maximum of the diffraction peak and θ is the Bragg angle. All values of the Scherrer equation were expressed in radians and FWHM was estimated using Jade 5.0.

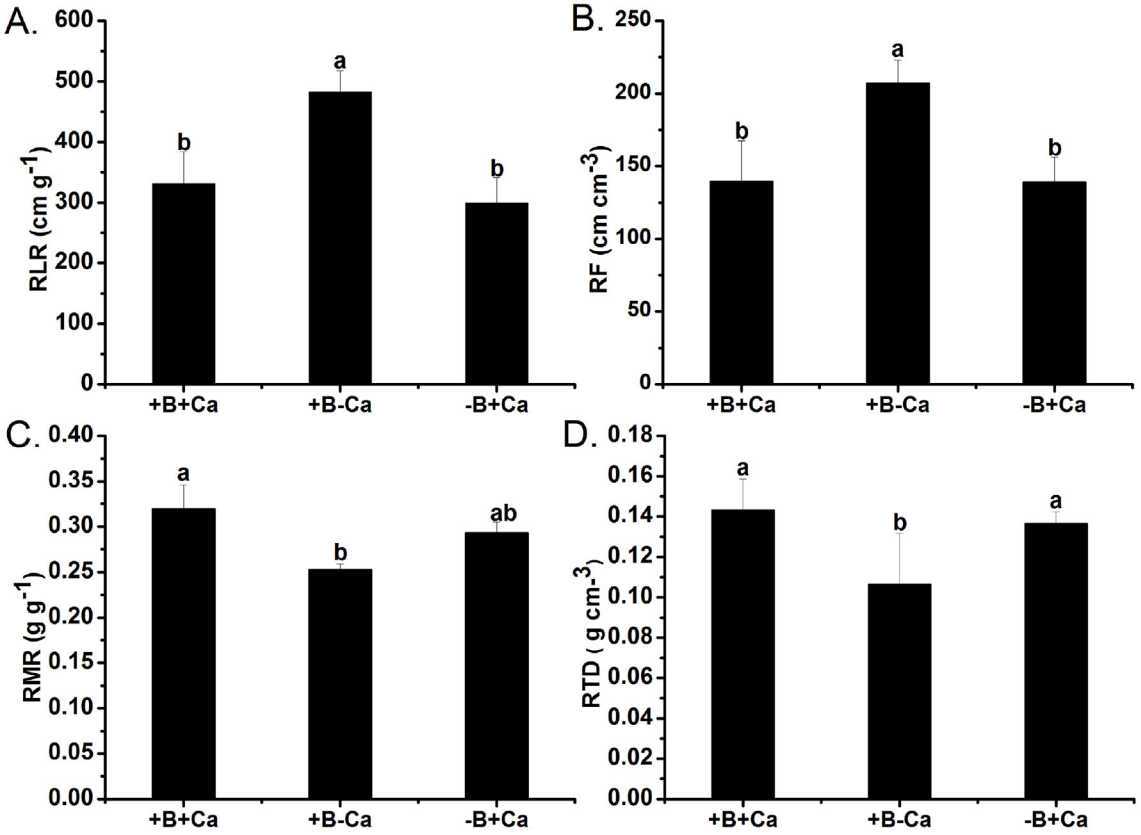

Fig. 3. Effect of B or Ca deficiency treatment on the evaluation of root growth of trifoliate rootstock (*Poncirus trifoliate* L.). +B + Ca: control, +B–Ca: Ca deficiency, -B + Ca: B deficiency. RLR: Root length ratio, RF: root fineness, RMR: root mass ratio, RTD: root tissue density. Different lowercase letters in the figure indicate a significant difference among three treatments at $P < 0.05$ level with mean ± SD (Duncan's multiple comparison test).

Table 1
Correlations of root parameters under + B + Ca treatment.

	RLR	RMR	RF	RTD	TRL	TSA	RFs	RV	RAD
RLR	1								
RMR	−0.908	1							
RF	0.842	−0.991	1						
RTD	0.231	−0.619	0.719	1					
TRL	0.584	−0.189	0.054	−0.655	1				
TSA	0.968	−0.984	0.950	0.467	0.363	1			
RFs	0.999*	−0.888	0.818	0.189	0.619	0.957	1		
RV	−0.420	0.000	0.135	0.786	−0.982	−0.180	−0.459	1	
RAD	−0.146	−0.283	0.410	0.929	−0.888	0.105	−0.189	0.959	1

Note: Minus sign represents negative correlation. +B + Ca: control. *$P < 0.05$. RLR: root length ratio, RMR: root mass ratio, RF: root fineness, RTD: root tissue density, TRL: total root length, TSA: total surface area, RFs: root forks, RV: root volume, RAD: root average diameter.

Table 2
Correlations of root parameters under + B–Ca treatment.

	RLR	RMR	RF	RTD	TRL	TSA	RFs	RV	RAD
RLR	1								
RMR	1.000**	1							
RF	−1.000**	−1.000**	1						
RTD	−1.000**	−1.000**	1.000**	1					
TRL	−0.268	−0.268	0.268	0.268	1				
TSA	−0.337	−0.337	0.337	0.337	0.997*	1			
RFs	−0.500	−0.500	0.500	0.500	0.968	0.984	1		
RV	−0.383	−0.383	0.383	0.383	0.993	0.999*	0.991	1	
RAD	−0.361	−0.361	0.361	0.361	0.995	1.000*	0.988	1.000*	1

Note: Minus sign represents negative correlation. +B–Ca: Ca deficiency. **$P < 0.01$,*$P < 0.05$. RLR: root length ratio, RMR: root mass ratio, RF: root fineness, RTD: root tissue density, TRL: total root length, TSA: total surface area, RFs: root forks, RV: root volume, RAD: root average diameter.

Table 3
Correlations of root parameters under -B + Ca treatment.

	RLR	RMR	RF	RTD	TRL	TSA	RFs	RV	RAD
RLR	1								
RMR	0.705	1							
RF	0.825	0.181	1						
RTD	0.262	−0.500	0.761	1					
TRL	−0.943	−0.428	−0.966	−0.569	1				
TSA	−0.851	−0.228	−0.999*	−0.729	0.978	1			
RFs	−0.705	−1.000**	−0.181	0.500	0.428	0.228	1		
RV	−0.765	−0.082	−0.995	−0.822	0.936	0.989	0.082	1	
RAD	−0.810	−0.156	−1.000*	−0.778	0.959	0.997*	0.156	0.997*	1

Note: Minus sign represents negative correlation. -B + Ca: B deficiency. $^{**}P < 0.01$,$^{*}P < 0.05$. RLR: root length ratio, RMR: root mass ratio, RF: root fineness, RTD: root tissue density, TRL: total root length, TSA: total surface area, RFs: root forks, RV: root volume, RAD: root average diameter.

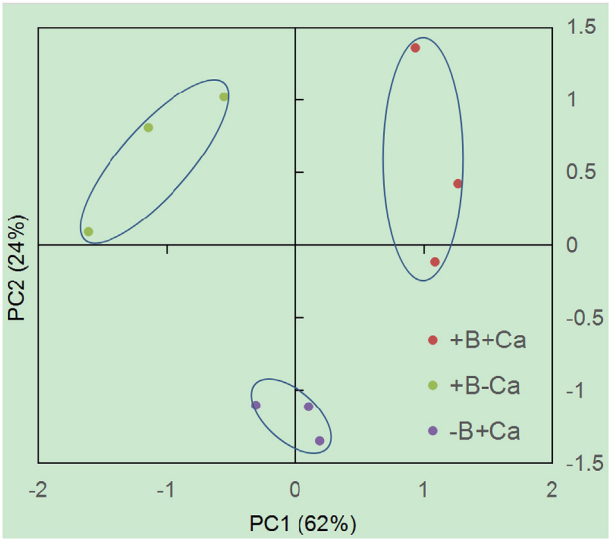

Fig. 4. The plot of the first two PC scores obtained by exploratory PCA of root growth parameters from different B and Ca treatments. +B + Ca: control, +B–Ca: Ca deficiency, -B + Ca: B deficiency.

2.6. Fourier transform infrared spectroscopy (FTIR) analysis of root CW

The powder of root CW (2 mg) was first mixed with KBr at the ratio of 1:100 (w/w), then the mixtures were pressed into transparent and uniform sheets by a tabletting machine. All the spectra (4000-400 cm^{-1}) were recorded by a VERTEX 70 spectrometer with an average of 64 scans at a resolution of 4 cm^{-1}. Normalized and baseline-corrected spectra from cell walls with B and Ca treatments were used for digital subtraction. Digital subtraction spectra of the averaged spectra representing control plant CW s minus that of B-deficient or Ca-deficient plant cell walls. (Liu et al., 2014).

2.7. Immunolocalisation of HG epitopes in root CW

For the immunohistochemical of HG epitopes, the methods of Yang et al. (2008) and Shi et al. (2017) were adopted. Briefly, one-month-old seedlings were cultured in hydroponic under B or Ca deficiency treatments. After 21 days treatment, fresh root tips were cut with a slicer within the root zone (2 mm) and directly collected into a fixation solution (containing 4% paraformaldehyde, 50 mM PIPES, 5 mM EGTA, 5 mM $MgSO_4$, pH 6.9). After 1 h of fixation at room temperature, samples were washed repeatedly with phosphate-buffered saline (PBS, three times) and then blocked with 0.2% bovine serum albumin (BSA) in PBS for 30 min. Then, the samples were incubated in primary monoclonal antibodies JIM5 (low methyl-esterified pectin) and JIM7 (high methyl-esterified pectin, those two primary monoclonal antibodies were purchased from University of Georgia (CCRC: Complex Carbohydrate Research Center, Georgia, USA), diluted 1:10 in PBS containing 0.2% BSA, for 2 h. Subsequently, samples were washed three times in PBS and incubated in goat anti-rat IgG (whole molecule) fluorescein isothiocyanate conjugate, diluted 1:50 in PBS containing 0.2% BSA for 2 h at 37 °C. Samples were washed with PBS three times and mounted on glass slides then examined under a laser-scanning confocal microscope (Olympus FV 1000,excitation wavelength:480 nm, emission wavelength:525 nm), frequencies of the circular hollow roots was calculated by area of the inner circle and area of the outer circle ratio.

2.8. Statistical analysis

Data processing and analysis among treatments were operated by one-way analysis of variance (ANOVA), and correlation analysis and principal component analysis (PCA) followed by Duncan's multiple comparisons using SPSS 20.0 package. OMNIC software was used for spectral normalization and baseline correction by FTIR, and all figures were generated by Origin pro 8.6 (Origin Lab Corporation, USA).

3. Results

3.1. Plant growth characteristics

The imbalance between B and Ca homeostasis in trifoliate rootstock significantly affected plant FW and DW (Fig. 1). The + B–Ca significantly decreased the FW of root, stem, and leaves by 47%, 50%, and 62%, respectively (Fig. 1A, B, C) compared to + B + Ca treatment. The treatment of -B + Ca only reduced root FW (Fig. 1A). However, in Ca-untreated plants, DW of root and leaves was significantly reduced (Fig. 1D, F); stem DW was lower but not significant. B deficiency decreased root DW relative to + B + Ca treatment (Fig. 1D), but the stem and leaves DW were not always to a significant level (Fig. 1E and F).

3.2. Root morphological parameters

Both + B–Ca and -B + Ca treatments had significant effects on root morphological parameters (Fig. 2). Compared with +B + Ca treatment, Ca deprivation caused a significant reduction in the TRL, TSA, RFs, RV, and RAD by 30%, 35%, 36%, 54%, and 24%, respectively. B deprivation decreased the TRL, TSA, RFs, RV by 41%, 29%, 51% and 36%, respectively. However, B deprivation did not reduce the RAD in contrast with +B + Ca. the results described above means that the imbalance of B and Ca homeostasis in the trifoliate rootstock had a significant impact on root growth.

3.3. Evaluation of root growth

Root length ratio (RLR), root fineness (RF), root mass ratio (RMR), root tissue density (RTD) are useful traits for evaluation of root growth

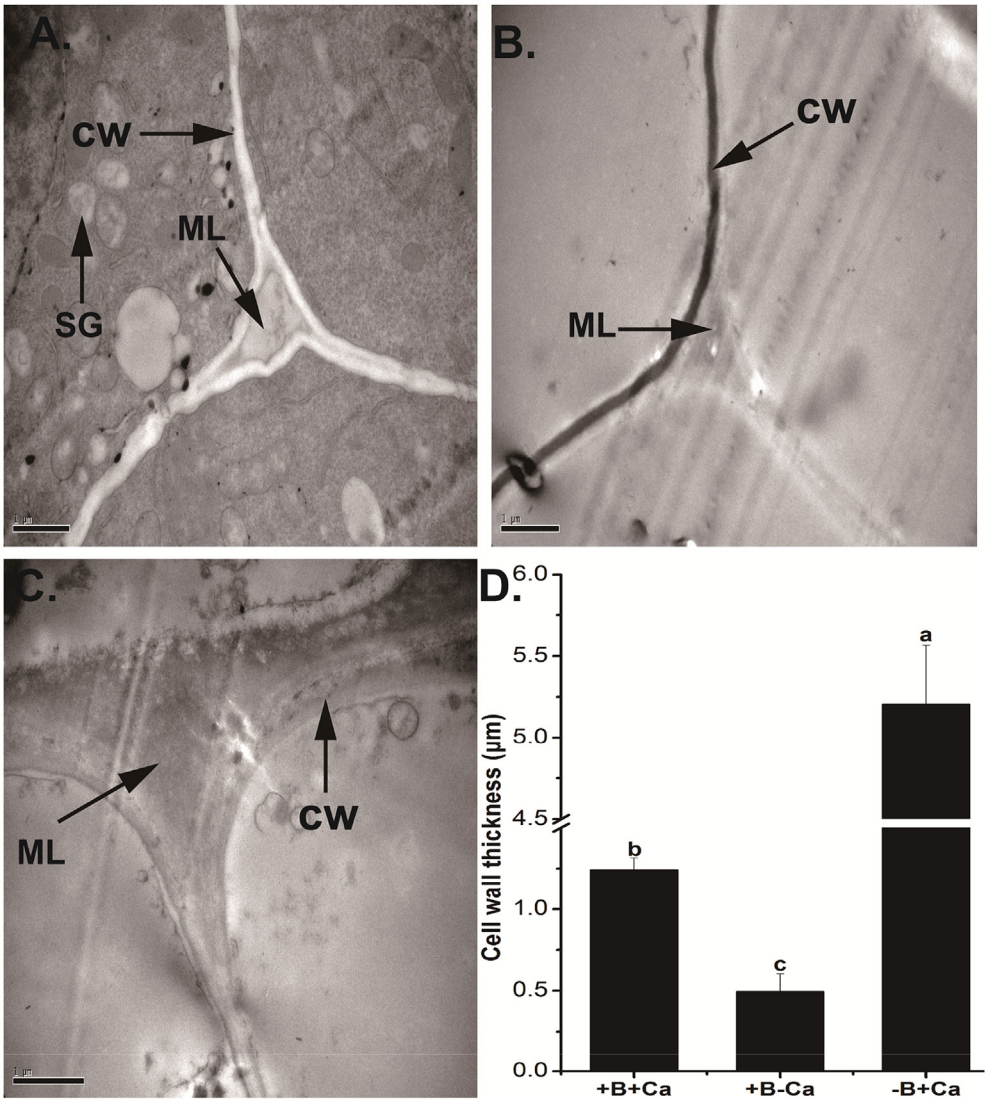

Fig. 5. Transmission electron micrograph of trifoliate rootstock (*Poncirus trifoliate* L.) cell wall that were exposed to + B + Ca (A), +B–Ca (B), -B + Ca (C) treatments and cell wall thickness (D). Transverse root section shown the clearly delineated middle lamella (ML), cell wall (CW), and starch grain (SG). Scale bar = 1 μm +B + Ca: control, +B–Ca: Ca deficiency, -B + Ca: B deficiency. Different lowercase letters in the figure indicate a significant difference among three treatments at $P < 0.05$ level with mean ± SD (Duncan's multiple comparison test).

(Fig. 3). In our experiment, +B–Ca treatment significantly increased the RLR and RF values at the ratio of 46% and 48%, respectively. While the two values of -B + Ca did not significantly differ compared to + B + Ca (Fig. 3A and B). Unlike RLR and RF, RMR and RTD were inhibited at the treatment of +B–Ca by 22% and 21% in contrast to + B + Ca treatment (Fig. 3C and D).

3.4. Correlation analysis and PCA of root growth parameters

Pearson correlation statistics were performed to analyze the difference of correlation between root parameters under B and Ca deficiency. For + B + Ca treatment, except for the positive correlation between RLR and RFs, there was no significant correlation among root system parameters (Table 1). There was a significant positive correlation among TSA, TRL, RV, and RAD ($p < 0.05$), and between RMR and RLR, RTD and RF, RAD and RV ($p < 0.01$), while correlation among RF and RLR, RMR ($p < 0.01$), RTD and RLR, RMR ($p < 0.01$) was significant negative under Ca deficiency (Table 2). For B deprivation, RAD was positively correlated with TSA, and RV ($p < 0.05$) and the relationship between RFs and RMR ($p < 0.01$), RF and TSA, RAD ($p < 0.05$) was negative (Table 3). The differences of the above correlations indicated that the effects of B and Ca deficiency on root growth allocation were different.

PCA divided all (9) quantitative traits into two principal components which showed 86% of the total variation (Fig. 4), it meant that the two components can explain these differences clearly. The first component accounted for 62% of total variation comprised of TSA, RV, RTD, RMR, RAD, and RLR, which represented root morphological development under B deficiency. The second component described 24% of the total variation and included TRL, and RFs, which were of evaluation of root elongation under Ca deficiency (Fig. 4; Supplemental Tables 1 and 2). The results showed that there were different changes in root growth parameters under B and Ca deficiency.

3.5. Visualization of CW by TEM

The changes of root subcellular structure were observed by TEM. Compared with +B + Ca, the TEM microphotographs showed that both + B–Ca and -B + Ca resulted in changes on CW architecture (Fig. 5A, B, C). The CW thickness was significantly decreased by 60% under + B–Ca treatment, while thickened root CW was more intense in -B + Ca, reaching a level to 319% in contrast to + B + Ca (Fig. 5D). In

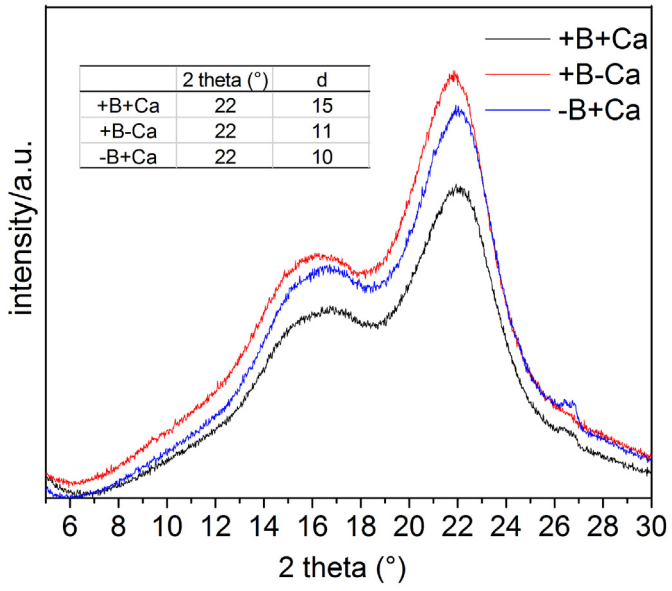

	2 theta (°)	d
+B+Ca	22	15
+B-Ca	22	11
-B+Ca	22	10

Fig. 6. X-ray diffraction pattern of CW samples of trifoliate rootstock (*Poncirus trifoliate* L.) under B or Ca deficiency treatment.

addition, starch grains were widely distributed in +B + Ca, and starch grains content were significantly reduced by B or Ca deficiency (Fig. 5B and C). Meanwhile, we found that the extraction rate of CW in B-deficient treatment was significantly increased, while that in Ca-deficient treatment significantly decreased (Supplemental figure 1).

3.6. XRD analysis of root CW

Cellulose crystalline structure of root CW samples after B or Ca deprivation treatment was observed by the X-ray diffraction patterns (Fig. 6). The reflection at 2θ = 15.4° corresponding to the superposition of (1$\bar{1}$0) and (110) planes and the peak at 2θ = 22.7° (200) plane are the characteristics for cellulose I crystal. The peaks at 2θ = 12.3° (1$\bar{1}$0), 20.3° (110) and 22.1° (200) planes are characteristic for cellulose II crystal (Yan and Gao, 2008). However, there was no significant peak intensity shift in these locations when compared with +B + Ca, while crystallite sizes were decreased significantly by + B–Ca or -B + Ca in contrast to + B + Ca. Therefore, we concluded that B or Ca deficiency had no evident effect on the relative intensity of the peak curve.

3.7. FTIR analysis of CW

FTIR spectroscopy was performed on CW samples to monitor resulting changes (Fig. 7A). Main and research-related absorption bands are related to the presence of functional chemical groups like carbohydrates, proteins, amides, and CW polysaccharides (cellulose, hemicellulose, pectin) (Supplemental Table 3). The intensity of the adsorbed band (3394 cm^{-1}) mainly N–H stretching for proteins intensified the bandwidths, and peak value at 3334 cm^{-1} (O–H and N–H stretching), 1130 cm^{-1} (β_{1-3} glucans and C–O–C stretching), 1065 cm^{-1} (β_{1-4} glucans and C–O and C–C stretching) for polysaccharides (cellulose, hemicellulose) showed no peak shift when compared to + B + Ca, while C–OH stretching at 1030 cm^{-1} about primary alcohols in cellulose significantly changed. The main characteristic peaks in 2927 cm^{-1} (C–H stretching), 1647 cm^{-1} (C=O stretching), 1425 cm^{-1} (C–N stretching), and 1248 cm^{-1} (C–N stretching and C–N–H stretching), were relative to proteins and amides (the major components of proteins) and were tended to shift their intensities. The bands that we assigned to pectin galactans were identified at 1734 cm^{-1}, 1485 cm^{-1} in both B and Ca deprivation (Liu et al., 2019b; Maria et al., 2019; Marianna et al., 2019).

The characteristic subtraction spectrum representing + B + Ca plant were relatively enriched with proteins and amides (3394, 2927, 1647, 1248, and 1020 cm^{-1}) and polysaccharides (1485 and 1030 cm^{-1}) were enhanced in B and Ca-deficient CWs. Interestingly, the negatively correlated peaks in B and Ca-deficient CWs were noticed.

3.8. Immunolocalisation of HG epitopes

The distribution of low and high-methyl esterified HG was studied by using JIM5 and JIM7 antibodies. Firstly, we observed that + B–Ca treatment resulted in circular hollow roots (frequency: 69%) through cross-section (Fig. 8 IV-VI). Compared with the control, the fluorescence density varied greatly under B and Ca deficiency conditions (Fig. 8). JIM7 localized HG brighter than JIM5 under Ca deficiency, indicating that the degree of methyl esterification of pectin was increased due to Ca deficiency, while immunolocalisation of JIM5 epitope under -B + Ca showed that low-methyl esterified HG was brighter than JIM7 under -B + Ca treatment (Fig. 8A).

4. Discussion

The well-developed root system is pivotal to take up nutrients, therefore root size and distribution are closely related to nutrient uptake capacity for plants including trifoliate rootstock seedlings (Forde and Lorenzo, 2001). Our study firstly analyzed the effects of B and Ca deficiency on biomass, root architecture and allocation. Both nutrients

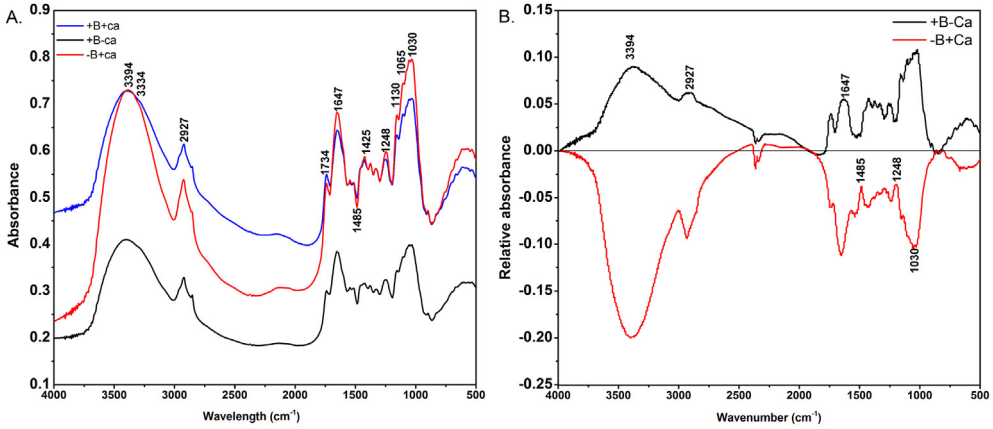

Fig. 7. Fourier-transform Infrared Spectroscopy spectra of treated cell wall in the range of 500–4000 cm^{-1}. (a). Characteristic peaks labelled for analysis (b). Spectra obtained by FTIR digital absorbance subtraction technique representing + B + Ca plant cell walls minus that of +B–Ca or -B + Ca plant cell wall.

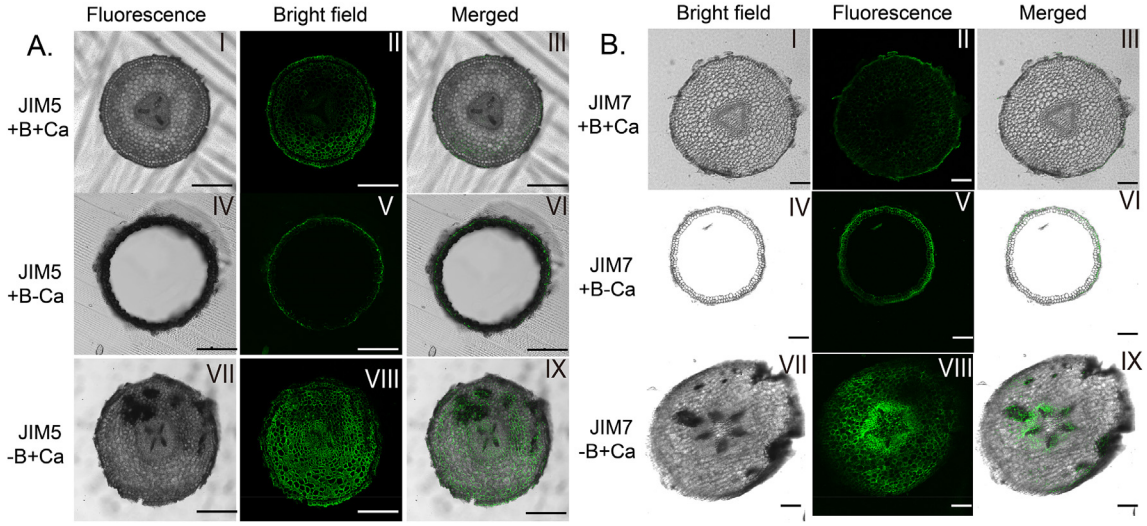

Fig. 8. Full image of fluorescent immunolocalisation of lowly methylesterified homogalaturonan epitope labelled with JIM5 (A) and highly methylesterified homogalacturonan epitope labelled with JIM7 (B) after B or Ca deficiency treatment in trifoliate rootstock (*Poncirus trifoliate* L.). Scale bar = 200 μm.

deprivations inhibited biomass of trifoliate rootstock, especially root FW and DW (Fig. 1), indicating that B or Ca deficiency inhibited the root growth of trifoliate rootstock seedlings.Some previous studies have shown that B and Ca deficiency change the root size and distribution, thereby inhibits root growth (Cao et al., 2013; Riaz et al., 2018).

Detailed morphological analysis was used to compare root growth under B or Ca deficiency treatment. In this study, parameters like TRL, TSA, RFs, and RV were decreased under both nutrient deficiencies (Fig. 2A, B, C, D), while only Ca deficiency significantly reduced RAD (Fig. 2E), same results were also observed in previous studies (Correia et al., 2003; González-Fontes et al., 2016: Liu et al., 2019b) indicating both nutrient deficiencies can inhibit root growth and worse performance of root system under B and Ca deficiencies surely inhibited the accumulation of trifoliate rootstock biomass (Fig. 1). Our research showed that Ca deficiency increased RLR and RF while decreased RMR and RTD to maintain root growth (Cao et al., 2013; Liu et al., 2019b). And this adjustment was defined as root morphological plasticity, which allows plants to adapt to Ca deficiency (Correia et al., 2003; Han et al., 2016). RTD was decreased significantly under the influence of Ca deficiency. RLR indicates the amount of plant biomass used for root development under stress conditions, which can be calculated with the equation: RLR = RMR*RF/RTD (Ryser and Lambers, 1995; Agostino et al., 2007). Our correlation analysis of Ca deficiency also quantitatively confirmed the results (Fig. 4). However, the effect of B deficiency on these parameters (RLR, RMR, RF, and RTD) was insignificant (Fig. 3). PCA combined with correlation analysis showed different inhibition ways under B and Ca deficiency, and interpretation of results demonstrated that B deficiency mainly inhibited root morphological development, while Ca deficiency mainly inhibited root elongation.

In the primary plant CW, cellulose is the main load-bearing component (mainly cellulose I, cellulose II) and hemicelluloses act as a water-holding matrix (Dolan et al., 2018). Besides, hemicelluloses influence the orientation and binding of cellulose fibers and are responsible for adjusting the microstructures of cellulose subnetworks (Johnson et al., 2018). The adhesion strength between cellulose fibers, cellulose, and the surrounding polymer matrix is the key factor to determine network mechanics (Grace et al., 2019). The primary CWs of higher plants contain more than 30% pectin polysaccharides. Pectin forms a hydrated gel phase and embeds in the network of cellulose microfibrils and other CW components. Covalent and non-covalent interactions between pectin polysaccharides and other CW components contribute to structural and functional stability of the CW (Levesque-Tremblay et al., 2015).

Ca deficiency reduced the CW thickness and extraction rate in relative to control (Fig. 5B, D; Supplemental figure 1), indicating Ca deprivation loosened the CW (Demarty et al., 1984) and then led to intracellular material outflow and CW degradation (Fig. 5B). Previous studies shown that Ca plays an essential role in determining the structure and function of the CW (Hepler, 2005) by cross-linking low methyl esterified pectin (Guillemin et al., 2008) in the cell wall to form a semi rigid pectate gel (Braccini and Perez, 2001), indicating that the degradation of CW may be related to the change of pectin. Previous studies has shown that B is mainly exsisted in the CW (Blevins and Lukaszewski, 1998). B forms boratediol ester bonds by crosslinking two RG-II chains in pectin (Funakawa and Miwa, 2015). The B-RG-II complex, exerting a mechanical function on the CW, is important for CW formation (Dumont et al., 2014). In our experiment, B deficiency increased CW thickness and extraction rate to maintain CW structure when compared to control (Fig. 5C and D; Supplemental figure 1), these results were consistent with our previous studies (Wu et al., 2017). Different changes of CW structure suggested that the effects of B and Ca deficiency on CW are not the same.

XRD was applied to detect the crystallinity of root CW to provide information about the polymorphic structure of cellulose (Szymańska-Chargot et al., 2019). Those reflections previously reported for cellulose I (15.4°, 22.7°) and cellulose II (12.3°, 20.3°, 22.1°) was observed no enhanced peak intensity and conversion of cellulose I to cellulose II (Fig. 6), indicating that cellulose did not occur significant change during both nutrient deficiencies, the result is similar to the report by Hernández-Hernández et al. (2016). However, crystallite sizes were reduced from 15 to 11 (+B–Ca) and 10 (-B + Ca), perhaps due to B and Ca deficiency resulted in the release of cellulose from pectic substances (Cárdenas-Pérez et al., 2018). Those above results suggested that changes in root CW structure may be mainly due to changes in pectin.

Additionally, FTIR spectra provide insight into functional groups of root CW. The band related to cellulose showed a small sharp difference at 1030 cm^{-1}, other related groups remained unchanged when compared to + B + Ca under B or Ca deficiency treatment, which could be explained by XRD data of reduced crystallite sizes. In addition, under + B–Ca treatment, the band corresponding to proteins, amides and pectins were all enhanceded in contrast to + B + Ca, this may be due to the release of large amounts of protein and amino acids from CW under B deficiency, previous study confirmed that B could connect the membrane with the cell wall through cross-linking glycosylinositol phosphorylcer amides of arabinogalactan proteins (Voxeur and Fry, 2014). Under the condition of Ca deficiency, the vibration peaks of

protein and amides decreased (Fig. 7), which is consistent with previous studies (Liu et al., 2019a). indicating B or Ca deficiency mainly alter those three constituents in CW, then the root growth was inhibited. (Wu et al., 2017; Butler et al., 2017; Dong et al., 2018).

It has been demonstrated that pectin profile and the degree and pattern of methyl-esterification of the HG pectin substructure are important in cell adhesion (Willats et al., 2001). Ca mainly binds with low methyl-esterified HG in pectin for forming the egg-box structure to maintain CW stability (Barbara et al., 2018). In the present study, low level of low methyl esterified pectin and enhanced level of high methyl esterified pectin were observed (recognized by JIM5 and JIM7, respectively) under + B–Ca treatment, indicating a low ability for intercellular adhesion leading to CW degradation. Pectin enriched in JIM5 epitopes is crucial to maintain CW adhesion (Corral-Martínez et al., 2019). JIM7 localized HG brighter than JIM5 under Ca deficiency, indicating that the methyl esterification degree of pectin increased due to Ca deficiency. This is not conducive to low methyl esterified pectin interacts with Ca maintaining the stability of the cell wall structure (Guillemin et al., 2008), which may be the reason for the rapid formation of hollow roots. While JIM5 localized HG brighter than JIM7 under B deficiency, This may facilitate the presence of low methyl esterified pectin to cross-linking Ca for maintaining CW structure (Guillemin et al., 2008), while this result was inconsistent with previous studies conducted by Riaz et al. (2018).

5. Conclusion

Based on our findings, we demonstrated that B and Ca deficiency all inhibited root growth, but their mechanisms are different. B deficiency can promote the formation of more low methyl esterified pectin to increase cell wall thickness, and then affect the morphological development of root system, while the formation of more highly methyl esterified pectin to increase cell wall degradation under Ca deficiency, which inhibited root elongation and formation of root branches. In addition, cellulose had not significantly changed under these two elements deficiencies.

Yalin Liu and Cuncang Jiang designed and supervised this study; Yalin Liu and Lei Yan conducted the experiments, performed data interpretation, and drafted the manuscript; Riaz Muhammad helped to revise the manuscript grammatically; Yu Zeng helped in replacing nutrition solution and determined related parameters. All authors read and approved the final manuscript.

Funding

This work was supported by the National Natural Science Foundation of China (41271320) and the Fundamental Research Funds for the Central Universities (2017PY055).

Declaration of competing interest

The authors declare that they have no conflict of interest.

Appendix A. Supplementary data

Supplementary data to this article can be found online at https://doi.org/10.1016/j.plaphy.2019.10.007.

References

Agostino, S., Abenavoli, M.R., Gringeri, P.G., Cacco, G., 2007. Comparing morphological plasticity of root orders in slow- and fast-growing citrus rootstocks supplied with different nitrate levels. Ann. Bot. 100 (6), 1287–1296.

Agustín, G.F., M Teresa, N.G., Camacho-Cristóbal, J.J., M BegoA, H.R., Carlos, Q.P., Jesús, R., 2014. Is Ca^{2+} involved in the signal transduction pathway of boron deficiency? new hypotheses for sensing boron deprivation. Plant Science s 217–218 (1), 135–139.

Ali, S., Xu, Y.Y., Ahmad, I., Jia, Q.M., Ma, X.C., Ullah, H., Alam, M., Adnan, M., Daurd, I., Ren, X.L., Cai, T., Zhang, J.H., Jia, Z.K., 2018. Tillage and deficit irrigation strategies to improve winter wheat production through regulating root development under simulated rainfall conditions. Agric. Water Manag. 209, 44–54.

Barbara, C., Ewa, S., Agata, L., Strubińska, J., 2018. Modification of pectin distribution in sunflower (*Helianthus annuus* L.) roots in response to lead exposure. Environ. Exp. Bot. 155, 251–259.

Bastías, E., Alcaraz-López, C., Bonilla, I., Martínez-Ballesta, M.C., Bola os, L., Carvajal, M., 2010. Interactions between salinity and boron toxicity in tomato plants involve apoplastic calcium. J. Plant Physiol. 167 (1), 0–60.

Bénédicte, C., Hervé, R., Bernard, B., 2019. Gazing at cell wall expansion under a golden light. Trends Plant Sci. 24, 2.

Blevins, D.G., Lukaszewski, K., 1998. Boron in plant structure and function. Annu. Rev. Plant Physiol. Plant Mol. Biol. 49, 481–500.

Braccini, I., Perez, S., 2001. Molecular basis of Ca^{2+} induced gelation in alginates and pectins: the eggbox model revisited. Biomacromolecules 2, 1089–1096.

Brown, P.H., Bellaloui, N., Wimmer, M.A., Bassil, E.S., Ruiz, J., Hu, H., 2002. Boron in plant biology. Plant Biol. 4 (2), 205–223.

Butler, H.J., Adams, S., Mcainsh, M.R., Martin, F.L., 2017. Detecting nutrient deficiency in plant systems using synchrotron fourier-transform infrared microspectroscopy. Vib. Spectrosc. 90, 46–55.

Cao, X., Chen, C., Zhang, D., Shu, B., Xiao, J., Xia, R., 2013. Influence of nutrient deficiency on root architecture and root hair morphology of trifoliate orange (*Poncirus trifoliata* L. raf.) seedlings under sand culture. Sci. Hortic. 162, 100–105.

Cárdenas-Pérez, S., Chanona-Perez, J.J., Güemes-Vera, N., Cybulska, J., Szymanska-Chargot, M., Chylinska, M., 2018. Structural, mechanical and enzymatic study of pectin and cellulose during mango ripening. Carbohydr. Polym. 196, 313–321.

Corral-Martínez, P., Driouich, A., Seguí-Simarro, J.M., 2019. Dynamic changes in arabinogalactan-protein, pectin, xyloglucan and xylan composition of the cell wall during microspore embryogenesis in *Brassica napus*. Front. Plant Sci. 10, 332.

Correia, P.J., Pestana, M., Martins-Loução, M.A., 2003. Nutrient deficiencies in carob (*Ceratoniasiliqua* L.) grown in solution culture. J. Hortic. Sci. Biotechnol. 78 (6), 847–852.

Demarty, M., Morvan, C., Thellier, M., 1984. Calcium and the cell wall. Plant Cell Environ. 7, 441–448.

Dolan, G.K., Yakubov, G.E., Stokes, J.R., 2018. Bio-tribology and bio-lubrication of plant cell walls. In: Roberts, J.A. (Ed.), Annual Plant Reviews Online. John Wiley & Sons.

Dong, X.C., Lu, X.P., Wu, X.W., Liu, G.D., Yan, L., Riaz, M., Wu, L.S., Jiang, C.C., 2018. Changes in chemical composition and structure of root cell wall of citrus rootstock seedlings in response to boron deficiency by FTIR spectroscopy. J. Hortic. Sci. Biotechnol. 93 (2), 150–158.

Dumont, M., Lehner, A., Bouton, S., Kiefer-Meyer, M.C., Voxeur, A.A., Pelloux, J., Lerouge, P., Mollet, J.C., 2014. The cell wall pectic polymer rhamnogalacturonan-II is required for proper pollen tube elongation: implications of a putative sialyltransferase-like protein. Ann. Bot. 114, 1177–1188.

Forde, B., Lorenzo, H., 2001. The nutritional control of root development. Plant Soil 232, 51–68.

Funakawa, H., Miwa, K., 2015. Synthesis of borate cross-linked rhamnogalacturonan II. Front. Plant Sci. 6, 223.

Goldbach, H.E., Yu, Q., Wingender, R., Schulz, M., Wimmer, M., Findeklee, P., 2015. Rapid response reactions of roots to boron deprivation. J. Plant Nutr. Soil Sci. 164 (2), 173–181.

González-Fontes, A., Herrera-Rodríguez, M.B., Martín-Rejano, E.M., 2016. Root responses to boron deficiency mediated by ethylene. Front. Plant Sci. 6, 1103.

Grace, K.D., Ben, C., Mauricio, R.B., Michael, J.G., Jason, R.S., Gleb, E.Y., 2019. Probing adhesion between nanoscale cellulose fibres using AFM lateral force spectroscopy: the effect of hemicelluloses on hydrogen bonding. Carbohydr. Polym. 208, 97–107.

Guillemin, A., Guillon, F., Degraeve, P., Rondeau, C., Devaux, M.F., Huber, F., Badel, E., Saurel, R., Lahaye, M., 2008. Firming of fruit tissues by vacuum-infusion of pectin methylesterase: visualisation of enzyme action. Food Chem. 109 (2), 368–378.

Han, P.P., Qin, L., Li, Y.S., Liao, X.S., Xu, Z., Xu, X.J., Xie, L.H., Liao, H., liao, X., 2016. Effects of different nutrient deficiencies on growth and root morphological changes of rapeseed seedlings (*Brassica napus* l.). Chin. J. Oil Crop Sci. 38 (1), 88–97 (In Chinese).

Hepler, P.K., 2005. Calcium: a central regulator of plant growth and development. The Plant Cell 17, 2142–2155.

Hernández-Hernández, H.M., Chanona-Pérez, J.J., Vega, A., Ligero, P., Farrera-Rebollo, R.R., Mendoza-Pérez, J.A., 2016. Spectroscopy and microscopy study of peroxyformic pulping of agave waste. Microsc. Microanal. 22, 1084–1097.

Herrera, M.B., 2013. Boron deficiency increases the levels of cytosolic Ca^{2+} and expression of Ca^{2+}-related genes in arabidopsis thaliana roots. Plant Physiol. Biochem. 8 (11), 55–60.

Hoagland, D.R., Arnon, D.I., 1950. The Water Culture Method for Growing Plants without Soil, vol. 374 California Agriculture Experimental Station, Circular.

Hu, H., Brown, P.H., 1994. Localization of boron in cell walls of squash and tobacco and its association with pectin - evidence for a structural role of boron in the cell wall. Plant Physiol. 105, 681–689.

Ishii, T., Matsunaga, T., 2001. Rhamnogalacturonan II is covalently cross-linked to homogalacturonan. Phytochemistry 57, 969–974.

Jiang, C.C., Wang, Y.H., Liu, G.D., Xia, Y., Peng, S.A., Zhong, B.L., 2009. Effect of boron on the leaves etiolation and fruit fallen of newhall navel orange. Plant Nutr. Fert. Sci. 15, 656–661.

Johnson, K.L., Gidley, M.J., Bacic, A., Doblin, M.S., 2018. Cell wall biomechanics: a tractable challenge in manipulating plant cell walls fit for purpose!. Curr. Opin. Biotechnol. 49, 163–171.

Kobayashi, M., Matoh, T., Azuma, J., 1996. Two chains of rhamnogalacturonan II are cross-linked by borate-diol ester bonds in higher plant cell walls. Plant Physiol. 110

(3), 1017–1020.
Konno, H., Nakashima, S., Maitani, T., Katoh, K., 2010. Alteration of pectic polysaccharides in cell walls, extracellular polysaccharides, and glycan-hydrolytic enzymes of growth-restricted carrot cells under calcium deficiency. Physiol. Plant. 107 (3), 287–293.
Kunhikrishnan, A., Thangarajan, R., Bolan, N.S., Xu, Y., Naidu, R., 2016. Functional relationships of soil acidification, liming, and greenhouse gas flux. Adv. Agron. 139, 1–71.
Levesque-Tremblay, G., Pelloux, J., Braybrook, S.A., Müller, Kerstin, 2015. Tuning of pectin methylesterification: consequences for cell wall biomechanics and development. Planta 242 (4), 791–811.
Liu, G., Dong, X., Liu, L., Wu, L., Peng, S.A., Jiang, C.C., 2014. Boron deficiency is correlated with changes in cell wall structure that lead to growth defects in the leaves of navel orange plants. Sci. Hortic. 176, 54–62.
Liu, K., Li, Q.M., Zha, X.Q., Pan, L.H., Bao, L.J., Zhang, H.L., Luo, J.P., 2019a. Effects of calcium or sodium ions on the properties of whey protein isolatelotus root amylopectin composite gel. Food Hydrocolloids 87, 629–636.
Liu, Y.L., Riaz, M., Wu, X.W., Yan, L., Du, C.Q., Jiang, C.C., 2019b. Boron and calcium homeostasis effects on trifoliate rootstock (*Poncirus trifoliata)* root configuration and nutrient utilization. Int. J. Agric. Biol. 21, 359–366.
María, C.P., Margarita, P.J., Josefa, L.M., Francisco, M.A., 2017. Amelioration of boron toxicity in sweet pepper as affected by calcium management under an elevated CO_2 concentration. Environ. Sci. Pollut. Res. 24, 10893–10899.
Maria, H.G., Canteri, C.M.G.C., Renard, C.L.B., Sylvie, B., 2019. ATR-FTIR spectroscopy to determine cell wall composition: application on a large diversity of fruits and vegetables. Carbohydr. Polym. 212, 186–196.
Marianna, F., Rossana, D.A., Alessandra, A., Raffaella, B., Silvia, D.S., Francesca, M., Sara, Z., 2019. Active rearrangements in the cell wall follow polymer concentration during postharvest withering in the berry skin of *Vitis vinifera* cv. Corvina. Plant Physiology and Biochemistry 135, 411–422.
Martín-Rejano, E.M., Camacho-Cristóbal, J.J., Herrera-Rodríguez, M.B., Rexach, J., Navarro-Gochicoa, M.T., González-Fontes, A., 2011. Auxin and ethylene are involved in the responses of root system architecture to low boron supply in arabidopsis seedlings. Plant Physiol. 142 (2), 170–178.
O'Neill, M., Albersheim, P., Darvill, A., 1990. The pectic polysaccharides of primary cell walls. Methods Plant Biochem. 2, 415–441.
O'Neill, M.A., Ishii, T., Albersheim, P., Darvill, A.G., 2004. Rhamnogalacturonan II: structure and function of a borate cross-linked cell wall pectic polysaccharide. Annu. Rev. Plant Biol. 55 (1), 109–139.
Piñero, M.C., Pérez-Jiménez, M., López-Marín, J., Amor, F.M.D., 2017. Amelioration of boron toxicity in sweet pepper as affected by calcium management under an elevated CO_2, concentration. Environ. Sci. Pollut. Control Ser. 24 (11), 10893–10899.
Quiles-Pando, C., Rexach, J., Navarro-Gochicoa, M.T., Camacho-CristÃbal, J.J., Herrera-RodrÃguez, M.B., GonzÃlez-Fontes, A., 2013. Boron deficiency increases the levels of cytosolic Ca^{2+} and expression of Ca^{2+}-related genes in *Arabidopsis thaliana* roots. Plant Physiol. Biochem. 8 (11), 55–60.
Redondo-Nieto, M., Maunoury, N., Mergaert, P., Kondorosi, E., Bonilla, I., Luis, B.Ã., 2012. Boron and calcium induce major changes in gene expression during legume nodule organogenesis. does boron have a role in signalling? New Phytol. 195 (1), 14–19.
Riaz, M., Lei, Y., Wu, X.W., Saddam, H., Omar, A., Jiang, C.C., 2018. Boron deprivation induced inhibition of root elongation is provoked by oxidative damage, root injuries and changes in cell wall structure. Environ. Exp. Bot. 156, 74–85.
Ryser, P., Lambers, H., 1995. Root and leaf attributes accounting for the performance of fast and slow-growing grasses at different nutrient supply. Plant Soil 170, 251–265.
Shi, D.C., Wang, J., Hu, R.B., Zhou, G.K., O'Neill, M.A., Kong, Y.Z., 2017. Boron-bridged RG-II and calcium are required to maintain the pectin network of the Arabidopsis seed mucilage ultrastructure. Plant Mol. Biol. 94 (3), 267–280.
Siddiqui, M.H., Al-Whaibi, M.H., Sakran, A.M., Ali, H.M., Basalah, M.O., Faisal, M., 2013. Calcium-induced amelioration of boron toxicity in radish. J. Plant Growth Regul. 32 (1), 61–71.
Szymanska-Chargot, M., Chylinska, M., Gdula, K., Kozioł, A., Zdunek, A., 2017. Isolation and characterisation of cellulose from different fruit and vegetable pomaces. Polymers 9 (495), 2–16.
Szymańska-Chargot, M., Chylińska, M., Pieczywek, P.M., Zdunek, A., 2019. Nanocellulose structure depending on the origin. Example of apple parenchyma and carrot root celluloses. Carbohydr. Polym. 210, 186–195.
Tan, L., Eberhard, S., Pattathil, S., Warder, C., Mohnen, D., 2013. An arabidopsis cell wall proteoglycan consists of pectin and arabinoxylan covalently linked to an arabinogalactan protein. The Plant Cell 25 (1), 270–287.
Tariq, M., Mott, C.J.B., 2007. Effect of applied calcium-boron ratio on the accumulation of nutrient-elements by radish (*Raphanus sativus* L.). J. Agricul. Biol. Sci. 2, 2.
Tuteja, N., 2009. Integrated calcium signaling in plants. Signaling in plants. In: Mancuso, S., Balusx¿ka, F. (Eds.), Signaling in Plants. Signaling and Communication in Plants. Springer, Berlin, Heidelberg, pp. 29–49.
Voxeur, A., Fry, S.C., 2014. Glycosylinositol phosphorylcer amides from Rosa cell cultures are boron bridged in the plasma membrane and form complexes with rhamnogalacturonan II. Plant J. 79, 139–149.
Willats, W.G.T., Orfila, C., Limberg, G., Buchholt, H.C., Van Alebeek, G.J., Voragen, A.G.J., 2001. Modulation of the degree and pattern of methylesterification of pectic homogalacturonan in plant cell walls: implications for pectic methyl esterase action, matrix properties and cell adhesion. J. Biol. Chem. 276, 19404–19413.
Wu, X.W., Riaz, M., Yan, L., Du, C.Q., Liu, Y.L., Jiang, C.C., 2017. Boron deficiency in trifoliate orange induces changes in pectin composition and architecture of components in root cell walls. Front. Plant Sci. 8, 1882.
Yamauchi, T., Hara, T., Sonoda, Y., 1986. Effects of boron deficiency and calcium supply on the calcium metabolism in tomato plant. Plant Soil 93 (2), 223–230.
Yan, L., Gao, Z., 2008. Dissolving of cellulose in PEG/NaOH aqueous solution. Cellulose 15, 789–796.
Yang, J.L., Li, Y.Y., Zhang, Y.J., Zhang, S.S., Wu, Y.R., Zheng, W.S.J., 2008. Cell wall polysaccharides are specifically involved in the exclusion of aluminum from the rice root apex. Plant Physiol. 146 (2), 602–611.